Energy Transfer in Near-Orthogonally Arranged Chromophores Separated through a Single Bond

ARTICLE *in* THE JOURNAL OF PHYSICAL CHEMISTRY C · MAY 2012

Impact Factor: 4.77 · DOI: 10.1021/jp303406p

THE JOURNAL OF PHYSICAL CHEMISTRY C

Article

pubs.acs.org/JPCC

Energy Transfer in Near-Orthogonally Arranged Chromophores Separated through a Single Bond

Rijo T. Cheriya,[†] Jimmy Joy,[†] Andrews P. Alex,[†] Anil Shaji,[‡] and Mahesh Hariharan*[,†]

[†]School of Chemistry and [‡]School of Physics, Indian Institute of Science Education and Research Thiruvananthapuram (IISER-TVM), CET Campus, Sreekaryam, Thiruvananthapuram, Kerala 695 016

Supporting Information

ABSTRACT: A combined experimental and theoretical study shows a significant barrier (ca. 100 kJ/mol) to rotation through the interchromophoric carbon−carbon single covalent (1.49 Å) bond between the naphthalenimide and perylenimide units that prevents coplanarization of the two units in the dyad **NP**, thereby forcing them to act as independent chromophores/redox centers. Upon photoexcitation, highly efficient energy transfer is observed from the naphthalenimide (energy donor) to the perylenimide (energy acceptor) moiety predominantly through Coulombic coupling, completely isolating the orbital overlap (Dexter-type) interaction between the chromophoric units at such short separation by virtue of their orthogonal arrangement. Because Förster's ideal-dipole approximation ignores the contribution from significant higher-order Coulombic interactions at such short distances between donor and acceptor moieties, the complete coupling was computed from the transition densities, giving an estimate of the energy-transfer rate from the naphthalenimide donor to the perylenimide acceptor of $k_{ET} = 2.2 \times 10^{10}$ s^{-1}, in agreement with observations. Ultrafast excitation energy (ca. 40 ps, 90%) and electron (<0.5 ps, 10%) transfer from the singlet excited state of naphthalenimide to the perylenimide moiety competes with further delayed processes in the conjugate **NP**. Upon excitation at 345 nm, conjugate **NP** exhibits near-quantitative energy transfer in conjunction with solvent-polarity-dependent (solvatochromic) perylenimide fluorescence, resulting in a remarkable Stoke's shift of ca. 175−240 nm. Favorable photophysical properties such as high fluorescence quantum yield, wide excitation range, ultrafast energy transfer, marginal electron transfer, and large Stoke's shift make this conjugate a potential candidate for biological applications.

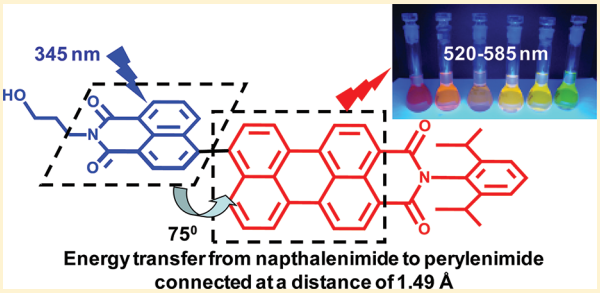

1. INTRODUCTION

Energy-transfer (ET) cassettes have gained immense importance during the past decade in the areas of DNA sequencing,[1,2] microscopic imaging,[3] artificial light-harvesting,[4−28] and biomolecular sensing,[29−43] among others. Electronic excitation energy transfer (EET) is the ubiquitous mechanism for energy transfer in multichromophoric systems.[44] EET mechanisms, characterized by their different distance dependences, include Förster-type[45] "Coulombic" interactions, Dexter-type exchange interactions,[46] and other contributions to short-range coupling due to orbital overlap effects.[47−52] Recently, coherent effects including interference between different EET mechanisms have also been of interest.[53,54] When orbital overlap between the chromophores is minimal, then the Dexter-type, through-bond interactions including exchange effects due to the indistinguishability of electrons are highly (exponentially) suppressed. Typically, when the chromophores are separated by more than 2−5 Å, orbital overlap effects can be ignored. At large separations, the dominant, through-space, Coulombic interaction is described by Förster theory wherein the electrostatic coupling is approximated by the dipole−dipole interaction between the chromophores. However, the ideal-dipole approximation (IDA) proposed by Förster to predict the rate of energy transfer in such cassettes breaks down at distances that are short compared to the size of the chromophores[55] because of higher-order interactions such as quadrupole−quadrupole and octupole−octupole interactions.

At relatively short separations between the chromophores, efficient energy transfer through the Dexter mechanism has been isolated and studied[2,56] in orthogonally aligned chromophoric dipoles (orientation factor, $\kappa^2 \approx 0$) for which Coulombic coupling is suppressed because of the perpendicular orientation. However, the electronic coupling for excitation energy transfer through predominant Coulombic interactions at short separations compared to the size of the chromophores, excluding the possibility of energy transfer through orbital overlap, has received less attention. Understanding mutually exclusive energy-transfer pathways at short separation is needed to yield better insight into coherence in quantum energy transfer.[53] Detailed analysis of such short-distance energy-transfer conjugates having negligible orbital overlap and the design of novel probes that combine solvatochromism[57]

Received: April 10, 2012
Revised: May 21, 2012

   dx.doi.org/10.1021/jp303406p | J. Phys. Chem. C XXXX, XXX, XXX−XXX

offering large Stoke's shift for biological applications[3,58,59] are of significant interest.

Herein, we report the synthesis and photophysical properties of a new candidate (extended 1,1′-binaphthyl derivative) to act as an energy-transfer conjugate (Figure 1) that can be

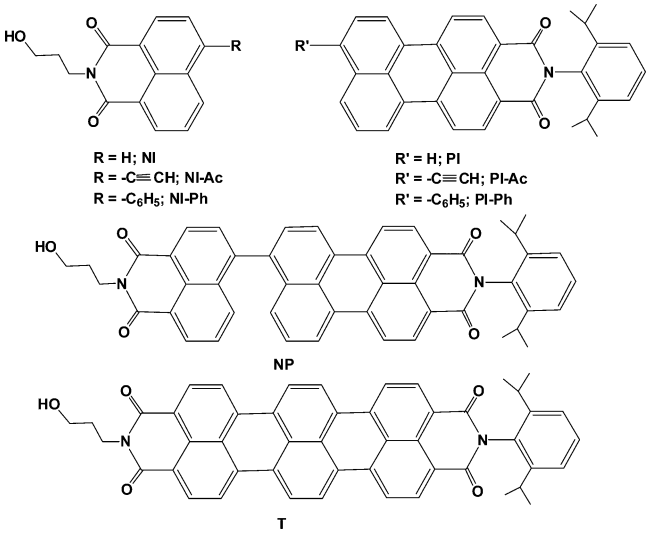

Figure 1. Structures of **NI**, **NI−Ac**, **NI−Ph**, **PI**, **PI−Ac**, **PI−Ph**, **NP**, and **T**.

conveniently incorporated into oligonucleotides or peptides. The present molecular system integrates naphthalenimide (energy donor) and perylenimide (energy acceptor; dipolar) moieties at the distance of a single covalent bond and enforces a sterically driven orthogonality between the two chromophores.[60] The perpendicular arrangement of the incorporated chromophores results in negligible orbital overlap, thereby isolating efficient energy-transfer effects through Coulombic interactions at short separations. By virtue of the dipolar nature of the perylenimide moiety and the possibility of exciting the naphthalenimide moiety (energy donor), this conjugate exhibits a remarkable pseudo-Stoke's shift of ca. 175−240 nm that is promising for biological applications.

2. EXPERIMENTAL SECTION

Electron-Transfer Rate and Energy-Transfer Rate. From the relative fluorescence quantum yields of the model derivative **PI** (Φ_{ref}) and conjugate **NP** (Φ) and the fluorescence lifetime of the model derivative **PI** (τ_{ref}) in toluene, an estimate of the rate constant of the electron-transfer process can be made as

$$k_{\text{electron transfer}} = \frac{(\Phi_{ref}/\Phi) - 1}{\tau_{ref}} \tag{1}$$

The changes in free energy for electron transfer from the singlet excited state of the naphthalenimide moiety to the perylenimide moiety and from the singlet excited state of the perylenimide moiety[61] to the naphthalenimide moiety were calculated using the Rehm−Weller equation[62,63]

$$\Delta G^0 = E_{ox}(D^{+\bullet}/D) - E_{red}(A/A^{-\bullet}) - E_{0,0} \tag{2}$$

where ΔG^0 is the change in free energy for photoinduced electron transfer, E_{ox} is the oxidation potential of the donor, E_{red} is the reduction potential of the acceptor, and $E_{0,0}$ is the singlet excited-state energy of the donor.

The electronic excitation energy-transfer rate according to the Förster theory is

$$k_{ET} = \frac{4\pi^2}{h^2 c}|V_{DA}|^2 J \tag{3}$$

where V_{DA} is the Coulombic coupling between the donor and acceptor expressed in wavenumbers. The spectral overlap, J, is given by the integral

$$J = \int G'_D(\nu) G_A(\nu) \mathrm{d}\nu \tag{4}$$

where

$$G'_D(\nu) = A\frac{g_D(\nu)}{\nu^3}, \quad G_A(\nu) = B\frac{g_A(\nu)}{\nu} \tag{5}$$

in which $g_D(\nu)$ and $g_A(\nu)$ are the donor emission and acceptor absorption spectra, respectively. A and B are constants that normalize the line shape functions G'_D and G_A to unit area in the wavenumber (ν) scale.[52]

To compute the EET rate, the coupling, V_{DA}, must be estimated along with the overlap integral. Let a denote the highest occupied molecular orbital (HOMO) of the donor and a' the corresponding lowest unoccupied orbital (LUMO), and let b and b' denote the same for the acceptor. The transition of interest that transfers the excitation from one chromophore to the other is between the state given by the Slater determinant $(|a\bar{a}'b\bar{b}| + |a'\bar{a}b\bar{b}|)/\sqrt{2}$ and the state given by $(|a\bar{a}'b\bar{b}| + |a\bar{a}b'\bar{b}|)/\sqrt{2}$, where a bar over a and b means that the corresponding orbital contains an electron with β spin; otherwise, the orbital is occupied by an α-spin electron. The interaction that transfers the excitation can therefore be formally written in its entirety as[44]

$$H_{\text{full}} = |\langle |a\bar{a}'b\bar{b}||\hat{H}||a\bar{a}b'\bar{b}|\rangle \tag{6}$$

In the absence of significant orbital overlap between the donor and acceptor, the leading contribution to the interaction is

$$\begin{aligned} H_{\text{full}} &\approx 2(aa'|bb') \\ &= 2\iint a'(r_1)b(r_2)\frac{1}{|r_1 - r_2|}a(r_1)b'(r_2)\mathrm{d}^3r_1\mathrm{d}^3r_2 \\ &\equiv V_{ed} \end{aligned} \tag{7}$$

where the integrals are over all space. The Coulomb interaction in eq 7 is between the two transition densities $P^{\text{donor}}_{aa'}(r_1)$ and $P^{\text{acceptor}}_{bb'}(r_2)$ and not between the electron clouds corresponding to each molecular orbital because the a and b orbitals do not overlap because of the orthogonality between the chromophores and orbitals a and a' (b and b') have no overlap with each other because they represent mutually orthogonal states. The transition density is the off-diagonal element of the quantum density matrix connecting the two electronic states of a molecule. One can think of the transition density as describing the deformation in the electronic cloud of a molecule when a transition occurs between two levels induced by either a real or a virtual photon. The interaction in eq 7 is the long-range Coulombic coupling between the transition densities by means of which the de-excitation of the energy donor resonates with the excitation of the acceptor. In terms of the transition densities, this electrodynamic interaction can be written as

dx.doi.org/10.1021/jp303406p | J. Phys. Chem. C XXXX, XXX, XXX−XXX

$$V_{ed} = \frac{e^2}{4\pi\varepsilon_0} \iint \frac{P_{aa'}^{donor}(r_1) P_{bb'}^{acceptor}}{|r_1 - r_2|} d^3r_1 d^3r_2 \quad (8)$$

When the separation between the donor and acceptor chromophores is large compared to their size, the resonant interaction between the transition densities is mediated by a real photon and in this case, the interaction can be approximated well by the dipole−dipole coupling between two ideal dipoles kept at the charge centers of the respective chromophores. However, when the separation is small compared to the size of the chromophores, the possibility of interactions mediated by virtual photons makes the ideal-dipole approximation inadequate. In the case of the conjugate **NP**, the orthogonal arrangement of the two chromophores minimizes orbital overlaps, making the EET mechanism dominantly Coulombic. However, the separation between the chromophores is only one covalent bond (1.49 Å), and the separation between their respective centers (∼7 Å) is comparable to the sizes of both **NI** and **PI**.

Because the ideal-dipole approximation cannot be used in the case of conjugate **NP**, the relevant transition densities for both **NI** and **PI** were computed using Qchem, and they were, in turn, used to compute V_{ed}. Numerically computed transition density cubes (TDCs) are not functions over space but rather values defined on a grid. The transition density values on the grid points are treated as integrals of the continuous transition density in eq 8 over cubes of volume $V_\delta = \delta x \delta y \delta z$, where δx, δy, and δz are the lattice constants defining the computational grid. During computation of the TDC elements, the sum is assumed to extend over spin dependencies, if any, of the continuous transition density. In terms of the TDC elements $M_D(i)$ and $M_{rmA}(j)$ of the donor and acceptor, respectively, one can write the electrodynamic component of EET as[64]

$$V_{ed} = \sum_{ij} \frac{M_D(i) M_A(j)}{4\pi\varepsilon_0 r_{ij}} \quad (9)$$

where r_{ij} is the separation between the ith lattice point of the donor's TDC and the jth lattice point of the acceptor's TDC.

3. RESULTS AND DISCUSSION

3.1. Synthesis and Structure of the Conjugate NP. N-subtituted 9-bromoperylenimide (**PI−Br**) was synthesized from perylene-3,4,9,10-tetracarboxylic anhydride through monoprotection using 2,6-diisopropylaniline and decarboxylation followed by bromination (Schemes S1−S3, Supporting Information), in accordance with the reported procedure.[20,65] The *N*-(hydroxypropyl)bromonaphthalenimide derivative was converted to the corresponding tributyltin derivative and further subjected to Stille coupling[66] with **PI−Br** to yield 50% of naphthalenimide−perylenimide conjugate **NP** (Schemes S1−S3). Model derivatives such as **NI−Ac**,[67] **NI−Ph**, **PI−Ac**,[68] **PI−Ph**, and **T**[69] were synthesized according to the reported procedures (see the Supporting Information).

As shown in Figure 2, the conjugate **NP** crystallizes in the triclinic space group $P\bar{1}$ with two molecules in the asymmetric unit (Table S1, Supporting Information). The conjugated nature of the individual chromophores was confirmed from the analysis of the crystal structure, with comparable bond lengths corresponding to conjugated carbon−carbon single and double bonds. However, the interchromophoric C−C bond length was found to be 1.49 Å, comparable to the C−C single bond length. The crystal structure of conjugate **NP** provides confirmation of this behavior, as it shows the naphthalenimide donor moiety to be twisted out of planarity by 75°. Consequently, the naphthalenimide and perylenimide units act as independent chromophores and not as a conjugated system. To understand the structure of dyad **NP** in solution, we carried out NMR experiments in $CDCl_3$. Two-dimensional ^1H NMR studies of conjugate **NP** in solution clearly revealed through-space interactions between the protons attached to (a) C43 and C20 and (b) C36 and C22 (Figure 2). No NOE coupling was observed between the protons attached to (a) C43 and C22 or (b) C43 and C23 (Figures S1−S9, Supporting Information). This further confirms the nonplanarity of the two constituent chromophoric units in conjugate **NP** in solution.

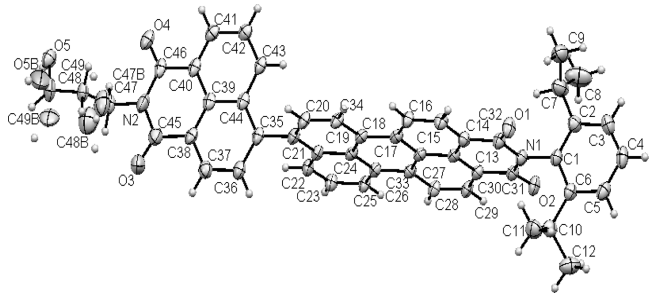

Figure 2. Crystal structure of the conjugate **NP**.

Furthermore, the extent of electronic interactions between the constituents **NI** and **PI** was understood through the examination of the electron density distributions in the frontier molecular orbitals (FMOs) of the constituents of the conjugate. The calculated electron density distributions in the frontier molecular orbitals (FMOs) of the constituents of the conjugate are shown in the Figure 3 and Figures S10−12 (Supporting Information). Inclusion of all four orbitals in each case is essential, as the transitions HOMO → LUMO and HOMO − 1 → LUMO + 1 are possible. Careful analysis of the FMOs clearly indicates that, for substituents that can be coplanar to **NI** and **PI** (e.g., acetylene-substituted **NI−Ac** and **PI−Ac**), the electron density is distributed in the substituent (acetylenyl) moiety in the LUMO (Figure S11, Supporting Information). Such delocalization results in a decrease in the energy difference between the HOMO and LUMO levels, as seen in the case of **PI−Ac** (4.12 eV), compared to **PI** (4.21 eV). In contrast, substituents such as phenyl (**PI−Ph**; 4.31 eV) and naphthalenimide (**NP**; 4.37 eV) moieties exhibit (Figure S12, Supporting Information and Figure 3) increases in the HOMO−LUMO gap. This could be attributed to large steric repulsion between hydrogen atoms, preventing rotation about the internuclear bond and leading to noncoplanar arrangements of the phenyl/perylenimide and naphthalenimide/perylenimide moieties.

3.2. Photophysical and Redox Properties of the Conjugate NP. Figure 4A shows the absorption spectra of the conjugate **NP** and the corresponding model chromophores **NI** and **PI** in acetonitrile. The absorption spectrum of conjugate **NP** is the sum of the absorption spectra of **NI** centered around 340 nm and **PI** centered around 480 nm, indicating that **NP** behaves as two separately conjugated chromophores connected through a single covalent bond. The ratio of molar extinction coefficients $\varepsilon_{PI}(507\ nm)/\varepsilon_{NI}(334\ nm)$ was found to be ca. 2.85 in the individual model chromophores, identical to that in the conjugate **NP** (Table S2, Supporting Information). A slight red shift (5−6 nm) in the band

dx.doi.org/10.1021/jp303406p | J. Phys. Chem. C XXXX, XXX, XXX−XXX

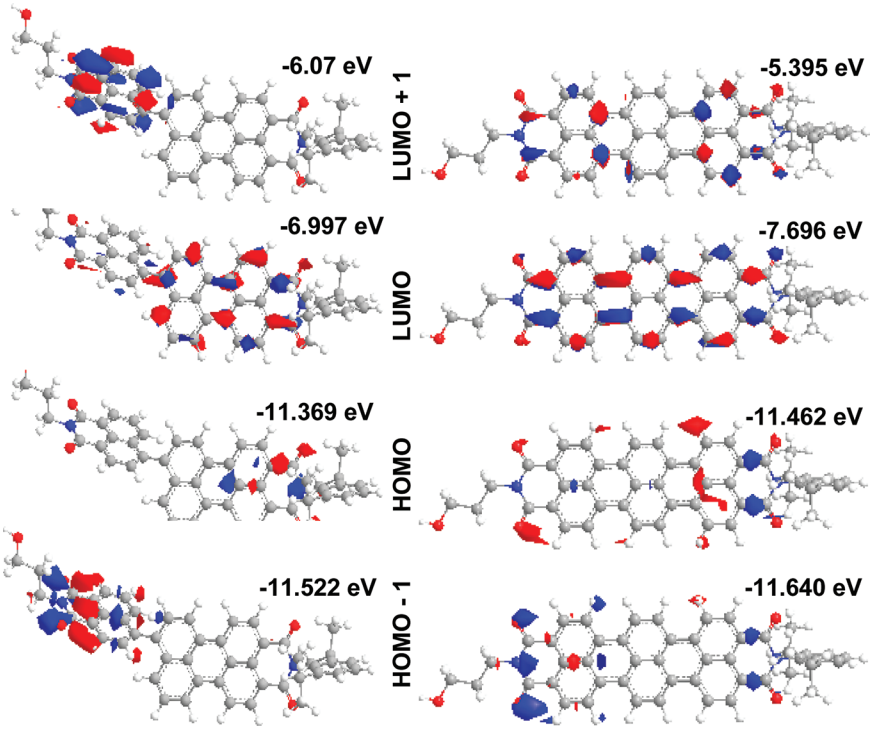

Figure 3. Electron density distributions and energies of the frontier molecular orbitals of the derivatives **NP** and its planar analogue **T**.

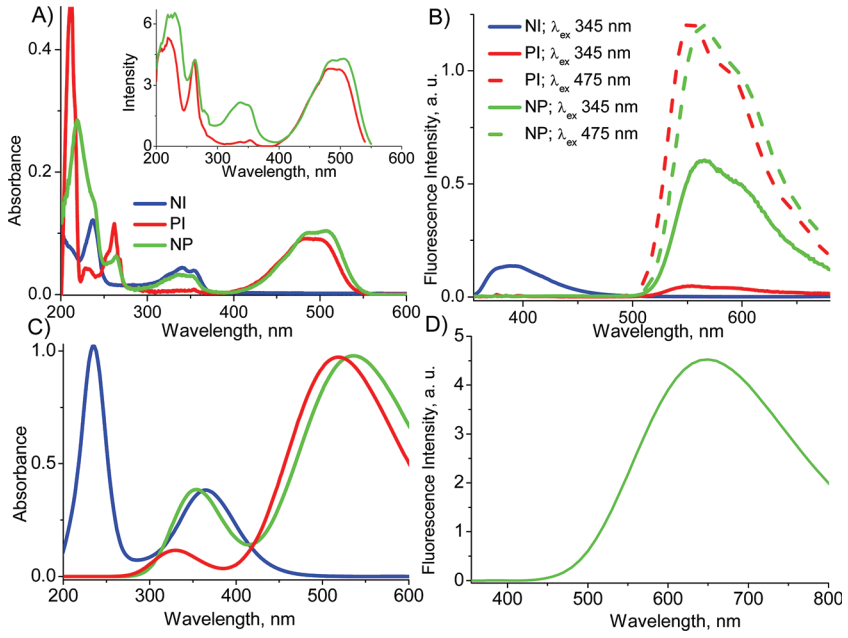

Figure 4. Experimental (A) absorption and (B) fluorescence emission spectra of **NI**, **PI**, and **NP** in acetonitrile and calculated (C) absorption spectra of **NI**, **PI**, and **NP** and (D) fluorescence emission spectrum of **NP** in acetonitrile. Inset in A: Excitation spectra of **PI** (red) and **NP** (green) in acetonitrile monitored at 553 nm.

corresponding to the perylenimide moiety of the conjugate **NP** indicates very weak electronic coupling between the constituents. Similar results were obtained for **NP** in nonpolar solvents such as cyclohexane and toluene and in polar solvents such as chloroform and methanol (Figures S13 and S14, Supporting Information).

The UV−vis spectra of the conjugate **NP** and the model derivatives **NI** and **PI** in acetonitrile solution were calculated using time-dependent density functional theory (TD-DFT)[70] at the B3LYP[71,72]/6-311G++(2d,2p) level associated with the polarized continuum model (PCM).[73] This method provides an accurate description of the UV−vis spectra of chromophoric systems.[74] Figure 4C shows the calculated UV−vis spectra of the derivatives **NI** and **PI** and the conjugate **NP** in acetonitrile. The absorption spectrum of **NI** in acetonitrile shows a broad band centered around 365 nm, nearly consistent with the experimental maximum of 340 nm. The absorption spectrum of **PI** in acetonitrile followed a similar discrepancy of 13 nm in the

dx.doi.org/10.1021/jp303406p | J. Phys. Chem. C XXXX, XXX, XXX−XXX

calculated maximum at 520 nm from the experimental data (507 nm). At the same time, conjugate **NP** in acetonitrile exhibited two bands that represent the sum of the absorption spectra of the model derivatives **NI** and **PI** in acetonitrile, with the ε_{PI}(520 nm)/ε_{NI}(365 nm) ratio as 2.7, in good agreement with the experimental data. Thus, a localized description of the individual components **NI** and **PI** is valid for the conjugate **NP**.

Figure 4B shows the fluorescence spectra of conjugate **NP** and the derivatives **NI** and **PI**. **NI**, the energy donor, has no emission in the wavelength range (500−700 nm), where the perylenimide moiety in **NP** and **PI** exhibits fluorescence. **PI**, the energy acceptor, excited at 345 nm, shows a very weak fluorescence, whereas conjugate **NP** strongly emits in the long-wavelength region (500−700 nm) corresponding to the perylenimide moiety when excited at 345 nm. At 345 nm, naphthalenimide can be excited with good selectivity (>95%), whereas above 420 nm, the perylenimide moiety absorbs exclusively (Table S2, Supporting Information). Whereas the energy acceptor **PI** absorbs feebly at 345 nm and gives a correspondingly weak fluorescence, conjugate **NP** exhibits energy transfer. Negligible fluorescence from the naphthalenimide (energy donor) moiety in **NP** is consistent with energy transfer to the acceptor perylenimide moiety. The fluorescence intensity of the perylenimide moiety through energy transfer (λ_{ex} = 345 nm) is less than that for the direct excitation (475 nm) of conjugate **NP**. Consistent with the absorption spectra, a red shift (9−10 nm) in the perylenimide emission band of the conjugate **NP** indicates a weak electronic coupling between the constituents. The quantum yield of **NP** was found to be ca. 0.81 ± 0.002, marginally lower than that of **PI** (Φ_F = 0.86 ± 0.002). TD-DFT calculation of the emission spectrum of **NP** conjugate (Figure 4D) resulted in the fluorescence emission only at the wavelength region corresponding to the perylenimide moiety, consistent with the experimental data. Upon excitation at both 345 and 475 nm, conjugate **NP** in ethanol at 77 K exhibited negligible phosphorescence,[28] similarly to the model derivative **PI** under similar conditions (Figure S15, Supporting Information). In contrast, the model derivative **NI** in ethanol at 77 K showed significant phosphorescence intensity centered around 540 nm upon excitation at 345 nm.[75]

The excitation spectrum of **NP** (inset of Figure 4A) monitored at 553 nm can clearly be superimposed on the absorption spectrum, confirming efficient energy transfer from the naphthalenimide to the perylenimide moiety. Similar extents of energy transfer were observed for **NP** in nonpolar solvents such as cyclohexane and toluene and in polar solvents such as chloroform and methanol (Figures S13 and S14, Supporting Information). Furthermore, conjugate **NP** exhibited strong solvent-polarity-dependent perylenimide emission upon excitation at 345 nm (Figure 5). A pseudo-Stoke's shift range of 165−240 nm was observed in varying solvents from cyclohexane (nonpolar) through methanol (polar). The solvatochromic behavior of conjugate **NP** can be attributed to the dipolar nature of the perylenimide moiety, in contrast to quadrupolar terrylene derivative **T** (Figure S16, Supporting Information), which exhibited a negligible Stoke's shift.

Moreover, the syntheses and photophysical characterizations of naphthalenimide- (**NI−Ac**, **NI−Ph**) and perylenimide- (**PI−Ac**, **PI−Ph**) based model derivatives containing extended conjugation such as acetylenyl and phenyl moieties were carried out. Acetylenyl and phenyl substituents were chosen because of their ability to (i) extend the conjugation and (ii) lower the barrier to rotation about the carbon−carbon bond at the

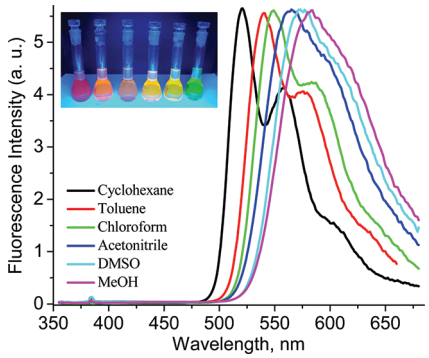

Figure 5. Solvent-polarity-dependent emission spectra of conjugate **NP** excited at 345 nm.

junction, unlike the naphthalenimide moiety in conjugate **NP**. Both the acetylenyl and phenyl derivatives exhibited red shifts in the absorption and emission spectra when compared to **NI** and **PI**, respectively (Figure S17, Supporting Information), consistent with the extent of conjugation and in good agreement with TD-DFT calculations (Figure S18, Supporting Information).

TD-DFT calculations clearly showed that the UV−vis spectrum of **PI−Ph** is significantly red-shifted compared to that of **PI** in acetonitrile, consistent with the experimental observation but in contrast to FMO analysis, whereas accurate descriptions of **NP** in acetonitrile are provided by both FMO analysis and TD-DFT calculations. Such consistency in the FMO and TD-DFT analyses of the conjugate **NP** can be attributed to the near-orthogonality of the chromophoric units, which results in the negligible perturbation of HOMO−LUMO levels. On the other hand, inconsistent FMO analysis of **PI−Ph** can be attributed to the static orthogonal geometry of the phenyl and perylenimide moieties resulting from the DFT method. Similar trends in FMO analyses and TD-DFT calculations were observed in the case of naphthalenimide derivatives. Interestingly, the minimum-energy conformer of conjugate **NP** was found to have a dihedral angle of 75° and a large barrier ($\Delta G \approx$ 100 kJ/mol)[60] to rotation through the internuclear bond between the naphthalenimide and perylenimide units that prevents coplanarization, consistent with the crystal structure of the conjugate **NP**. The model derivative terrylene **T** having an overall planar and conjugated structure exhibited a significantly lower HOMO−LUMO energy difference (3.766 eV). This is consistent with the observed absorption maximum centered on 651 nm, significantly red-shifted (by ca. 100 nm) compared to that of conjugate **NP** in acetonitrile (Figure S16, Supporting Information).

Figure 6 shows the fluorescence decay profiles of **NP** in various solvents monitored at 563, 549, and 521 nm in acetonitrile, chloroform, and cyclohexane, respectively, and excited at 340 and 439 nm. The singlet excited-state lifetime of conjugate **NP** in acetonitrile is found to be 4.2 ns when excited at 340 and 439 nm and monitored at 563 nm, which corresponds to singlet excited state of the perylenimide moiety (Table S3, Supporting Information). Whereas the lifetime of the model derivative **PI** under similar conditions exhibited a marginally longer lifetime of 5.1 ns, the fluorescence lifetime of **NI** is <0.005 ns.[25] The shorter singlet excited-state lifetimes of the perylenimide chromophore excited at both 340 and 439 nm in conjugate **NP** compared to model derivative **PI** further confirm a weak electronic perturbation in the perylenimide

dx.doi.org/10.1021/jp303406p | J. Phys. Chem. C XXXX, XXX, XXX−XXX

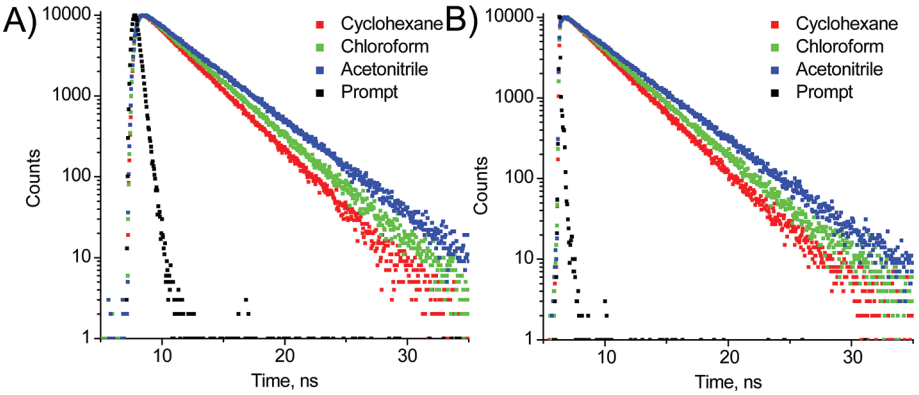

Figure 6. Fluorescence lifetimes of **NP** excited at (A) 340 and (B) 439 nm. Emission collected at 563, 549, and 521 nm for acetonitrile, chloroform, and cyclohexane, respectively.

moiety, in agreement with the steady-state absorption and emission spectra.

The afficiency of energy transfer from the naphthalenimide to the perylenimide moiety in conjugate **NP** was evaluated using the equation

$$\text{efficiency}\,(\%) = \frac{\Phi_{NP}}{\Phi_{PI}} \times 100 \qquad (10)$$

and was found to be 90%, where the quantum yield of **NP**, Φ_{NP}, was corrected for competitive absorption by the perylenimide moiety (ca. 5%) when excited at 345 nm. A similar high efficiency of energy transfer was achieved in an analogous donor–acceptor system but through the incorporation of four units of donor and one acceptor unit separated through a lengthy flexible spacer.[28] To understand the marginal loss in efficiency of energy transfer, we calculated the change in free energy for the electron-transfer reaction,[62,63] using redox potentials and the singlet excited-state energies of **NI** and **PI**[25] (Table 1). The change in free energy was found to be ΔG_{ET} = −0.17 eV for electron transfer from the singlet excited state of **NI** to **PI** and ΔG_{ET} = 0.44 eV from the singlet excited state of **PI** to **NI** in acetonitrile. As expected from the calculated changes in free energy for electron transfer from **NI** to **PI**, we observed a non-negligible loss of photons when conjugate **NP** was excited at 345 nm.

Table 1. Redox Potentials (Volts versus Ag/AgCl) of Conjugate NP and Derivatives NI and PI in $CH_3CN/CHCl_3$ Mixture

	E_{ox}	E_{red}	$E_{0,0}$
NI	2.26	−1.33	3.38
PI	1.49, 2.01	−0.95, −1.49	2.38
NP	1.48, 2.08, 2.27	−0.97, −1.33, −1.49	2.40

This clearly demonstrates that, upon excitation, the naphthalenimide moiety can undergo electron transfer to reduce the perylenimide moiety,[17] leading to the formation of the radical ion pair $N^{\bullet+}P^{\bullet-}$ and consequently decreasing the efficiency of energy transfer.[28] This marginal free energy change for favorable electron transfer from **NI** to **PI** is consistent with the decrease in the quantum yield of **NP** compared to that of **PI** in toluene. The radical anions of **NI**[75] and **PI**[25] are centered around 413 and 581 nm, respectively, whereas the radical cations of **NI** and **PI** exhibit very low molar extinction coefficients, as observed using spectroelectrochemical methods (Figures S19 and S20, Supporting Information). We observed no charge-separated species generated through electron transfer from the singlet excited state of naphthalenimide to the perylenimide moiety, $k_{electron\text{-}transfer} = 2.29 \times 10^{12}\ s^{-1}$ (Figure 7), in nanosecond flash photolysis studies, which can be attributed to fast charge recombination on the subnanosecond time scale.

We observed the decay (τ = 440 ns) of only the triplet excited state corresponding to the perylenimide moiety[17,22,68] in conjugate **NP** in toluene (Φ_T = 0.11) upon photoexcitation at 355 nm when monitored at 550 nm by nanosecond time-resolved absorption spectrometry (Figure 7C). In contrast, the photoexcitation of the model derivative **PI** in toluene at 355 nm showed a significantly lower triplet quantum yield (Φ_T = 0.08; τ = 960 ns) than the conjugate **NP** in toluene. The lower triplet quantum yield of **PI** in toluene can be attributed to reduced intersystem crossing to the triplet state, as in the case of the perylenediimide derivatives ($\Phi_T \approx 0.001$).[76,77] In addition, photoexcitation of model derivative **NI** in toluene under similar conditions exhibited the decay (τ = 650 ns) of the triplet-excited state of the naphthalenimide moiety when monitored at 470 nm (Φ_T = 0.49),[78] as reported earlier.

In Figure 8, the cyclic voltammogram of **NP** in $CH_3CN/CHCl_3$ is shown together with those of the model derivatives **NI** and **PI**. A comparison with the model derivatives reveals that the three reversible reduction waves of **NP** correspond to two reversible reductions of the **PI** moiety followed by one reduction of the **NI** moiety (Table 1). The oxidation of **NP** reveals three reversible peaks, which results from two reversible oxidation waves of the perylenimide unit and one reversible oxidation wave of the naphthalenimide unit (Table 1). From these measurements, it is evident that, for **NP**, the first reduction peak involves the formation of the perylenimide anion [E_0(**NP**/**NP**$^-$) = −0.97 V vs Ag/AgCl], whereas the first oxidation results in the perylenimide cation [E_0(**NP**/**NP**$^+$) = +1.48 V vs Ag/AgCl]. The energy difference between the oxidation and reduction of **NP** hence amounts to 2.45 eV, consistent with the difference in value for **PI** (2.44 eV). This clearly confirms that the identities of the two redox centers[79] are unperturbed in the conjugate **NP**, even though they are connected through a single covalent bond.

3.3. Energy and Electron Transfer from the Naphthalenimide to the Perylenimide Unit. In Figures 9 and 10, the strength of the electrodynamic coupling, V_{ed}, between **NI** and **PI** computed using their transition density cubes (TDCs) is shown. Figure 9 shows the dependence of the coupling on the torsional angle between the energy donor and acceptor

dx.doi.org/10.1021/jp303406p | J. Phys. Chem. C XXXX, XXX, XXX−XXX

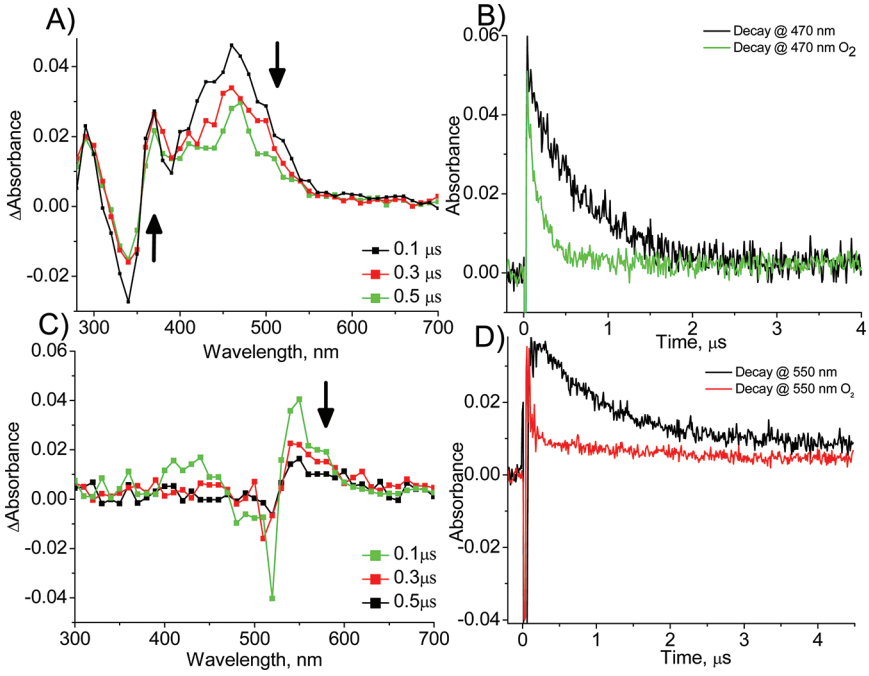

Figure 7. (A,C) Transient absorption spectra and (B,D) corresponding decay profiles of (A,B) **NI** and (C,D) **NP** in toluene. Excited at 355 nm.

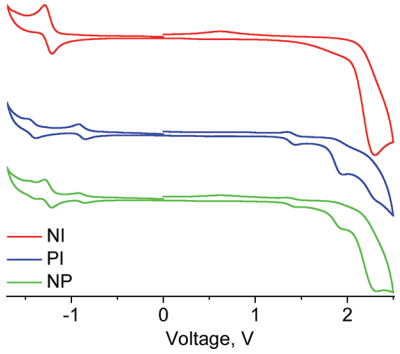

Figure 8. Cyclic voltammograms of **NI**, **PI**, and **NP** in a $CH_3CN/CHCl_3$ (3:2) mixture.

while the distance between them is kept constant at 1.49 Å. Figure 10 shows the dependence on the distance between the two chromophoric units while the torsional angle is kept equal to that of the conjugate **NP** (78°). The dipole−dipole

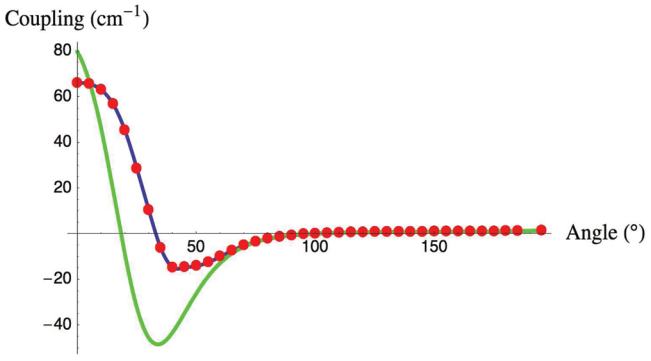

Figure 9. Torsional angle dependence on Coulombic coupling between naphthalenimide (energy donor) and perylenimide (energy acceptor). The green line shows the coupling computed using the ideal-dipole approximation.

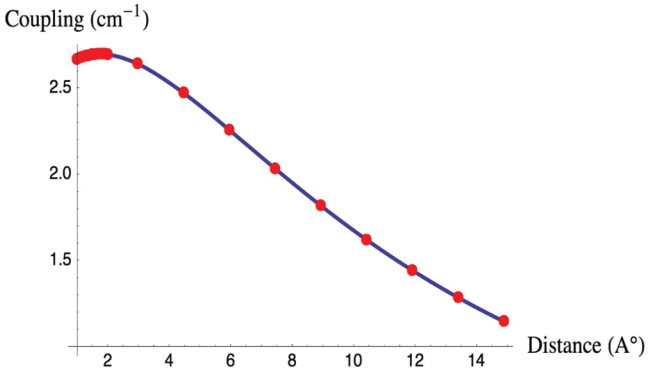

Figure 10. Distance dependence of Coulombic coupling between naphthalenimide (energy donor) and perylenimide (acceptor).

interaction is also shown in Figure 9 (green solid line) to illustrate the extent to which the ideal-dipole approximation fails to estimate the coupling between the two chromophores accurately. A deviation from R^{-6} in the distance and angular dependence of Coulombic coupling is clearly indicative of the existence of higher-order interactions between the naphthalenimide (donor) and perylenimide (acceptor) moeities. The results obtained from the TDC calculations indicate a strong coupling of 3.5 cm^{-1} and a rate of energy transfer of $k_{ET} = 2.2 \times 10^{10}$ s^{-1} from the naphthalenimide to the perylenimide moiety at a dihedral angle of 75° and a separation distance of 1.49 Å. The shallow nature of the twist potential (75° ± 15°) between the two chromophoric units can allow the dyad to adopt various conformers in solution, thereby resulting in different coupling strengths.

FMO analysis further supports the possibility of photoinduced electron and excitation ET. The fact that HOMO − 1 and LUMO + 1 of **NP** (electron density located on the donor naphthalenimide moiety) are bracketed outside the HOMO−LUMO gap of the conjugate **NP** (electron density located on the acceptor perylenimide moiety) accounts for the possibility

dx.doi.org/10.1021/jp303406p | J. Phys. Chem. C XXXX, XXX, XXX−XXX

of minimal radiative photoinduced electron transfer followed by nonradiative relaxation, that is, excitation energy transfer (Figure 11).[80−83] It is also apparent from the FMO calculations

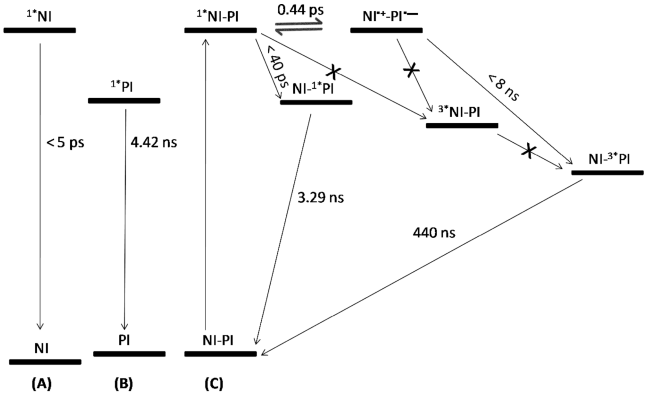

Figure 11. Energy level diagrams for (A) **NI** and (B) **PI** and **NP** (indicated for clarity as **NI−PI** in this scheme) in toluene excited at 355 nm.

that the orbitals involved in the electronic transitions are localized in the respective chromophores and, hence, the efficiency of energy transfer through orbital overlap is negligible.

The absence of the triplet state corresponding to the naphthalenimide moiety in conjugate **NP** is indicative of the fact that the ultrafast energy and electron-transfer processes are competing to prevent the population of alternate delayed processes such as phosphorescence. The significantly higher triplet quantum yield of conjugate **NP** corresponding to the perylenimide moiety compared to that of the model derivative **PI** suggests the possibility of recombination of the charge-separated state leading to the formation of triplet excited state as a possible pathway, as shown in Figure 11.[68] The absence of the triplet state and the phosphorescence corresponding to the naphthalenimide unit in conjugate **NP** rules out the possibility of the formation of the **PI** triplet state through Dexter-type energy transfer from naphthalenimide (donor) to perylenimide (acceptor) in conjugate **NP**. Thus, the overall efficiency in energy transfer (ca. 90%) can be attributed to predominant Coulombic interactions, with the remaining 10% efficiency dissipated through photoinduced electron transfer resulting in the formation of triplet state of perylenimide moiety. In view of the negligible orbital overlap between the electronic systems, the present work allows for the accurate quantification of the contributions from higher-order interactions to the overall Coulombic coupling for excitation energy transfer excluding other energy-transfer mechanisms.

By virtue of steric repulsion between interchromophoric hydrogens present in the conjugate **NP** (similar to that of the 1,1′-binaphthyl system), the conjugate assumes a near-orthogonal arrangement of the chromophoric subunits as confirmed from the crystal structure and two-dimensional NMR measurements. Despite being at the proximity of a carbon−carbon single covalent bond (1.49 Å), the orthogonal arrangement of chromophoric units makes the conjugate **NP** a combination of two independent chromophores/redox centers. Such behavior can be attributed to the poor orbital overlap of the two chromophoric units in the orthogonal arrangement. The identities of the two units were confirmed using UV−visible, fluorescence, and electrochemical studies. Excitation of the naphthalenimide (donor) moiety results in highly efficient energy transfer (90%) leading to fluorescence of the perylenimide moiety (acceptor). Excitation energy transfer (k_{ET} = 2.2 × 10^{10} s^{-1}) observed might be due to efficient spectral overlap and favorable dipole−dipole orientation (Figure S21, Supporting Information). Moreover, a minor pathway (<10%) of photoinduced electron transfer from the singlet excited state of the naphthalenimide to the perylenimide moiety (Figure 11) leads to a charge-separated state.

4. CONCLUSIONS

In conclusion, we have designed and synthesized a donor−acceptor conjugate at the separation distance of a single bond (1.49 Å). Sterically driven orthogonality retains the individuality of the two chromophores/redox centers, as confirmed through crystal structure, cyclic voltammetry, and photophysical studies. Upon photoexcitation at 345 nm, we observed efficient energy transfer from the naphthalenimide (donor) to the perylenimide (acceptor) moiety, leading to solvatochromic perylenimide fluorescence emission. The orthogonality of the chromophores enforced by the steric barrier allows the donor and acceptor moieties to be held at a distance of a single bond, maximizing Coulombic coupling and simultaneously nullifying any contribution from orbital overlap to energy transfer. Transition density cube (TDC) analysis showed strong Coulombic coupling between the transition densities of the napthalenimide and perylenimide moieties. Transient absorption studies and FMO analysis unequivocally suggest that energy transfer predominantly occurs by through-space interactions. Marginal radiative electron transfer, a high quantum yield (Φ = 0.81), a wide excitation range, and a large solvatochromic shift (240 nm) make the energy-transfer conjugate **NP** attractive for biological applications.[84] Further progress is underway in our laboratory to incorporate this conjugate in oligonucleotides.

■ ASSOCIATED CONTENT

Supporting Information

Synthesis details of **NI**, **PI**, **NI−Ac**, **NI−Ph**, **PI−Ac**, **PI−Ph**, **NP**, and **T**; absorption, fluorescence, and phosphorescence emission spectra of **NI**, **PI**, and **NP** under different conditions; spectroelectrochemical data; one- and two-dimensional ^{1}H NMR spectra; crystal data and structure refinement data of **NP** (in CIF format). This material is available free of charge via the Internet at http://pubs.acs.org.

■ AUTHOR INFORMATION

Corresponding Author

*Fax: (91)-471-2597427. E-mail: mahesh@iisertvm.ac.in.

Notes

The authors declare no competing financial interest.

■ ACKNOWLEDGMENTS

The authors thank the National Institute for Interdisciplinary Science and Technology (NIIST), Thiruvananthapuram, India, for generously extending their experimental facilities and Northwestern University for extending its crystal structure facility. The authors thank Professor Brent P. Krueger for providing Coupling6 software. M.H. acknowledges the Science and Engineering Research Board (SERB) for the support of this work, SERB/F/0962. A.S. acknowledges the Department of Science and Technology for partial support of this work

through the Ramanujan Fellowship and DST Fast-Track Scheme for Young Scientists, SERC sl. no. 2786.

REFERENCES

(1) Jiao, G. S.; Thoresen, L. H.; Kim, T. G.; Haaland, W. C.; Gao, F.; Topp, M. R.; Hochstrasser, R. M.; Metzker, M. L.; Burgess, K. *Chem.—Eur. J.* **2006**, *12*, 7816−7826.

(2) Wan, C.-W.; Burghart, A.; Chen, J.; Bergström, F.; Johansson, L. B. Å.; Wolford, M. F.; Kim, T. G.; Topp, M. R.; Hochstrasser, R. M.; Burgess, K. *Chem.—Eur. J.* **2003**, *9*, 4430−4441.

(3) Lin, W.; Yuan, L.; Cao, Z.; Feng, Y.; Song, J. *Angew. Chem., Int. Ed.* **2010**, *49*, 375−379.

(4) Schlichting, P.; Duchscherer, B.; Seisenberger, G.; Basché, T.; Bräuchle, C.; Müllen, K. *Chem.—Eur. J.* **1999**, *5*, 2388−2395.

(5) Moore, T. A.; Moore, A. L.; Gust, D. *Philos. Trans. R. Soc. London B* **2002**, *357*, 1481−1498.

(6) Metivier, R.; Kulzer, F.; Weil, T.; Muellen, K.; Basche, T. *J. Am. Chem. Soc.* **2004**, *126*, 14364−14365.

(7) Hinze, G.; Haase, M.; Nolde, F.; Muellen, K.; Basche, T. *J. Phys. Chem. A* **2005**, *109*, 6725−6729.

(8) Metivier, R.; Nolde, F.; Muellen, K.; Basche, T. *Phys. Rev. Lett.* **2007**, *98*, 047802.

(9) Fuckel, B.; Hinze, G.; Nolde, F.; Mullen, K.; Basche, T. *Phys. Rev. Lett.* **2009**, *103*, 103003.

(10) Curutchet, C.; Feist, F. A.; Averbeke, B. V.; Mennucci, B.; Jacob, J.; Mullen, K.; Basche, T.; Beljonne, D. *Phys. Chem. Chem. Phys.* **2010**, 12.

(11) Maus, M.; De, R.; Lor, M.; Weil, T.; Mitra, S.; Wiesler, U.-M.; Herrmann, A.; Hofkens, J.; Vosch, T.; Müllen, K.; De Schryver, F. C. *J. Am. Chem. Soc.* **2001**, *123*, 7668−7676.

(12) Gronheid, R.; Hofkens, J.; Kohn, F.; Weil, T.; Reuther, E.; Muellen, K.; De Schryver, F. C. *J. Am. Chem. Soc.* **2002**, *124*, 2418−2419.

(13) Cotlet, M.; Gronheid, R.; Habuchi, S.; Stefan, A.; Barbafina, A.; Muellen, K.; Hofkens, J.; De Schryver, F. C. *J. Am. Chem. Soc.* **2003**, *125*, 13609−13617.

(14) Maeda, C.; Kim, P.; Cho, S.; Park, J. K.; Lim, J. M.; Kim, D.; Vura-Weis, J.; Wasielewski, M. R.; Shinokubo, H.; Osuka, A. *Chem.—Eur. J.* **2010**, *16*, 5052−5061.

(15) Yoon, M.-C.; Yoon, Z. S.; Cho, S.; Kim, D.; Takagi, A.; Matsumoto, T.; Kawai, T.; Hori, T.; Peng, X.; Aratani, N.; Osuka, A. *J. Phys. Chem. A* **2007**, *111*, 9233−9239.

(16) Bahng, H. W.; Yoon, M.-C.; Lee, J.-E.; Murase, Y.; Yoneda, T.; Shinokubo, H.; Osuka, A.; Kim, D. *J. Phys. Chem. B* **2012**, *116*, 1244−1255.

(17) Kirmaier, C.; Song, H.-e.; Yang, E.; Schwartz, J. K.; Hindin, E.; Diers, J. R.; Loewe, R. S.; Tomizaki, K.-y.; Chevalier, F.; Ramos, L.; Birge, R. R.; Lindsey, J. S.; Bocian, D. F.; Holten, D. *J. Phys. Chem. B* **2010**, *114*, 14249−14264.

(18) Muthukumaran, K.; Loewe, R. S.; Kirmaier, C.; Hindin, E.; Schwartz, J. K.; Sazanovich, I. V.; Diers, J. R.; Bocian, D. F.; Holten, D.; Lindsey, J. S. *J. Phys. Chem. B* **2003**, *107*, 3431−3442.

(19) Langhals, H.; Saulich, S. *Chem.—Eur. J.* **2002**, *8*, 5630−5643.

(20) Langhals, H.; Jaschke, H.; Bastani-Oskoui, H.; Speckbacher, M. *Eur. J. Org. Chem.* **2005**, 4313−4321.

(21) Langhals, H.; Poxleitner, S.; Krotz, O.; Pust, T.; Walter, A. *Eur. J. Org. Chem.* **2008**, *2008*, 4559−4562.

(22) Hayes, R. T.; Walsh, C. J.; Wasielewski, M. R. *J. Phys. Chem. A* **2004**, *108*, 3253−3260.

(23) Kelley, R. F.; Goldsmith, R. H.; Wasielewski, M. R. *J. Am. Chem. Soc.* **2007**, *129*, 6384−6385.

(24) Gunderson, V. L.; Wilson, T. M.; Wasielewski, M. R. *J. Phys. Chem. C* **2009**, *113*, 11936−11942.

(25) Bullock, J. E.; Vagnini, M. T.; Ramanan, C.; Co, D. T.; Wilson, T. M.; Dicke, J. W.; Marks, T. J.; Wasielewski, M. R. *J. Phys. Chem. B* **2010**, *114*, 1794−1802.

(26) You, C.-C.; Hippius, C.; Grüne, M.; Würthner, F. *Chem.—Eur. J.* **2006**, *12*, 7510−7519.

(27) Sautter, A.; Kaletas, B. K.; Schmid, D. G.; Dobrawa, R.; Zimine, M.; Jung, G.; van Stokkum, I. H. M.; De Cola, L.; Williams, R. M.; Wuerthner, F. *J. Am. Chem. Soc.* **2005**, *127*, 6719−6729.

(28) Flamigni, L.; Ventura, B.; You, C.-C.; Hippius, C.; Wuerthner, F. *J. Phys. Chem. C* **2007**, *111*, 622−630.

(29) Kumar, M.; Kumar, N.; Bhalla, V.; Singh, H.; Sharma Parduman, R.; Kaur, T. *Org. Lett.* **2011**, *13*, 1422−1425.

(30) Jiao, G.-S.; Kim, T. G.; Topp, M. R.; Burgess, K. *Org. Lett.* **2004**, *6*, 1701−1704.

(31) Han, J. Y.; Loudet, A.; Barhoumi, R.; Burghardt, R. C.; Burgess, K. *J. Am. Chem. Soc.* **2009**, *131*, 1642−1643.

(32) Muthiah, C.; Kee, H. L.; Diers, J. R.; Fan, D.; Ptaszek, M.; Bocian, D. F.; Holten, D.; Lindsey, J. S. *Photochem. Photobiol.* **2008**, *84*, 786−801.

(33) Otsuki, J.; Kanazawa, Y.; Kaito, A.; Islam, D. M. S.; Araki, Y.; Ito, O. *Chem.—Eur. J.* **2008**, *14*, 3776−3784.

(34) Ren, X.-F.; Ren, A.-M.; Feng, J.-K.; Zhou, X. *Org. Electron.* **2010**, *11*, 979−989.

(35) Yang, J.-S.; Yan, J.-L.; Lin, C.-K.; Chen, C.-Y.; Xie, Z.-Y.; Chen, C.-H. *Angew. Chem., Int. Ed.* **2009**, *48*, 9936−9939.

(36) Kim, T. G.; Castro, J. C.; Loudet, A.; Jiao, J. G. S.; Hochstrasser, R. M.; Burgess, K.; Topp, M. R. *J. Phys. Chem. A* **2006**, *110*, 20−27.

(37) Eng, M. P.; Albinsson, B. *Angew. Chem., Int. Ed.* **2006**, *45*, 5626−5629.

(38) Eng, M. P.; Mårtensson, J.; Albinsson, B. *Chem.—Eur. J.* **2008**, *14*, 2819−2826.

(39) Langhals, H.; Esterbauer, A. J.; Walter, A.; Riedle, E.; Pugliesi, I. *J. Am. Chem. Soc.* **2010**, *132*, 16777−16782.

(40) Diring, S.; Ziessel, R.; Barigelletti, F.; Barbieri, A.; Ventura, B. *Chem.—Eur. J.* **2010**, *16*, 9226−9236.

(41) Curutchet, C.; Mennucci, B.; Scholes, G. D.; Beljonne, D. *J. Phys. Chem. B* **2008**, *112*, 3759−3766.

(42) Beljonne, D.; Pourtois, G.; Silva, C.; Hennebicq, E.; Herz, L. M.; Friend, R. H.; Scholes, G. D.; Setayesh, S.; Mullen, K.; Bredas, J. L. *Proc. Natl. Acad. Sci. U.S.A.* **2002**, *99*, 10982−10987.

(43) Agyin, J. K.; Morrison, H.; Siemiarczuk, A. *J. Am. Chem. Soc.* **1995**, *117*, 3875−3876.

(44) Scholes, G. D. *Annu. Rev. Phys. Chem.* **2003**, *54*, 57−87.

(45) Förster, T. *Naturwissenschaften* **1946**, *6*, 166−175.

(46) Dexter, D. L. *J. Chem. Phys.* **1953**, *21*, 836−850.

(47) Krueger, B. P.; Scholes, G. D.; Fleming, G. R. *J. Phys. Chem. B* **1998**, *102*, 5378−5386.

(48) Krueger, B. P.; Scholes, G. D.; Fleming, G. R. *J. Phys. Chem. B* **1998**, *102*, 9603−9604.

(49) Hsu, C.-P. *J. Phys. Chem. A* **2006**, *110*, 13640−13641.

(50) Hsu, C.-P.; You, Z.-Q.; Chen, H.-C. *J. Phys. Chem. C* **2008**, *112*, 1204−1212.

(51) Hsu, C.-P. *Acc. Chem. Res.* **2009**, *42*, 509−518.

(52) (a) Krueger, B. P. The role of carotenoids in bacterial light harvesting. Ph.D. Thesis, University of Chicago, Chicago, IL, 1999. (b) Sissa, C.; Terenziani, F.; Painelli, A.; Manna, A. K.; Pati, S. K. *Chem. Phys.* 2012, DOI: 10.1016/j.chemphys.2012.01.004.

(53) Scholes, G. D. *J. Phys. Chem. Lett.* **2010**, *1*, 2−8.

(54) Olaya-Castro, A.; Scholes, G. D. *Int. Rev. Phys. Chem.* **2011**, *30*, 49−77.

(55) Munoz-Losa, A.; Curutchet, C.; Krueger, B. P.; Hartsell, L. R.; Mennucci, B. *Biophys. J.* **2009**, *96*, 4779−4788.

(56) Jiao, G. S.; Thoresen, L. H.; Burgess, K. *J. Am. Chem. Soc.* **2003**, *125*, 14668−14669.

(57) Reichardt, C. *Solvents and Solvent Effects in Organic Chemistry*; VCH: Weinheim, Germany, 1988.

(58) Margineanu, A.; Hotta, J.-i.; Van der Auweraer, M.; Ameloot, M.; Stefan, A.; Beljonne, D.; Engelborghs, Y.; Herrmann, A.; Müllen, K.; De Schryver, F. C.; Hofkens, J. *Biophys. J.* **2007**, *93*, 2877−2891.

(59) Signore, G.; Nifosi, R.; Albertazzi, L.; Storti, B.; Bizzarri, R. *J. Am. Chem. Soc.* **2010**, *132*, 1276−1288.

(60) Meca, L.; Eha, D.; Havlas, Z. *J. Org. Chem.* **2003**, *68*, 5677−5680.

(61) Berlman, I. B. *Handbook of Fluorescence Spectra of Aromatic Molecules*; Academic Press: New York, 1971.
(62) Rehm, D.; Weller, A. *Ber. Bunsen-Ges. Phys. Chem.* **1969**, *73*, 834−836.
(63) Weller, A. Z. *Phys. Chem.* **1982**, *133*, 93−98.
(64) McWeeny, R.; Sutcliffe, B. T. *Methods of Molecular Quantum Mechanics*; Academic Press: London, 1969.
(65) Feiler, L.; Langhals, H.; Polborn, K. *Liebigs Ann.* **1995**, 1229−1244.
(66) Holtrup, F. O.; Müller, G. R. J.; Uebe, J.; Müllen, K. *Tetrahedron* **1997**, *53*, 6847−6860.
(67) McAdam, C. J.; Morgan, J. L.; Murray, R. E.; Robinson, B. H.; Simpson, J. *Aust. J. Chem.* **2004**, *57*, 525−530.
(68) Boixel, J.; Blart, E.; Pellegrin, Y.; Odobel, F.; Perin, N.; Chiorboli, C.; Fracasso, S.; Ravaglia, M.; Scandola, F. *Chem.—Eur. J.* **2010**, *16*, 9140−9153.
(69) Jung, C.; Ruthardt, N.; Lewis, R.; Michaelis, J.; Sodeik, B.; Nolde, F.; Peneva, K.; Müllen, K.; Bräuchle, C. *ChemPhysChem* **2009**, *10*, 180−190.
(70) Frisch, M. J.; Trucks, G. W.; Schlegel, H. B.; Scuseria, G. E.; Robb, M. A.; Cheeseman, J. R.; Montgomery, J. A., Jr.; Vreven, T.; Kudin, K. N.; Burant, J. C.; Millam, J. M.; Iyengar, S. S.; Tomasi, J.; Barone, V.; Mennucci, B.; Cossi, M.; Scalmani, G.; Rega, N.; Petersson, G. A.; Nakatsuji, H.; Hada, M.; Ehara, M.; Toyota, K.; Fukuda, R.; Hasegawa, J.; Ishida, M.; Nakajima, T.; Honda, Y.; Kitao, O.; Nakai, H.; Klene, M.; Li, X.; Knox, J. E.; Hratchian, H. P.; Cross, J. B.; Bakken, V.; Adamo, C.; Jaramillo, J.; Gomperts, R.; Stratmann, R. E.; Yazyev, O.; Austin, A. J.; Cammi, R.; Pomelli, C.; Ochterski, J. W.; Ayala, P. Y.; Morokuma, K.; Voth, G. A.; Salvador, P.; Dannenberg, J. J.; Zakrzewski, V. G.; Dapprich, S.; Daniels, A. D.; Strain, M. C.; Farkas, O.; Malick, D. K.; Rabuck, A. D.; Raghavachari, K.; Foresman, J. B.; Ortiz, J. V.; Cui, Q.; Baboul, A. G.; Clifford, S.; Cioslowski, J.; Stefanov, B. B.; Liu, G.; Liashenko, A.; Piskorz, P.; Komaromi, I.; Martin, R. L.; Fox, D. J.; Keith, T.; Al-Laham, M. A.; Peng, C. Y.; Nanayakkara, A.; Challacombe, M.; Gill, P. M. W.; Johnson, B.; Chen, W.; Wong, M. W.; Gonzalez, C.; Pople, J. A. *Gaussian 03*; Gaussian, Inc.: Wallingford, CT, 2003.
(71) Becke, A. D. *J. Chem. Phys.* **1993**, *98*, 5648−5652.
(72) Lee, C.; Yang, W.; Parr, R. G. *Phys. Rev. B* **1988**, *37*, 785−789.
(73) Miertus, S.; Scrocco, E.; Tomasi, J. *J. Chem. Phys.* **1981**, *55*, 117−129.
(74) Preat, J.; Jacquemin, D.; Wathelet, V.; Andre, J.-M.; Perpete, E. A. *J. Phys. Chem. A* **2006**, *110*, 8144−8150.
(75) Rogers, J. E.; Kelly, L. A. *J. Am. Chem. Soc.* **1999**, *121*, 3854−3861.
(76) Rachford, A. A.; Goeb, S. b.; Castellano, F. N. *J. Am. Chem. Soc.* **2008**, *130*, 2766−2767.
(77) Ford, W. E.; Kamat, P. V. *J. Phys. Chem.* **1987**, *91*, 6373−6380.
(78) Cho, D. W.; Fujitsuka, M.; Sugimoto, A.; Yoon, U. C.; Mariano, P. S.; Majima, T. *J. Phys. Chem. B* **2006**, *110*, 11062−11068.
(79) Veldman, D.; Chopin, S. p. M. A.; Meskers, S. C. J.; Janssen, R. A. J. *J. Phys. Chem. A* **2008**, *112*, 8617−8632.
(80) Sariciftci, N. S.; Smilowitz, L.; Heeger, A. J.; Wudl, F. *Science* **1992**, *258*, 1474−1476.
(81) Marcus, R. A. *Angew. Chem., Int. Ed.* **1993**, *32*, 1111−1121.
(82) Xu, Q. H.; Moses, D.; Heeger, A. J. *Phys. Rev. B* **2003**, *67*, 245417−245421.
(83) Bredas, J. L. *Chem. Rev.* **2005**, *104*, 4971−5004.
(84) Lakowicz, J. R. *Principles of Fluorescence Spectroscopy*, 3rd ed.; Springer: New York, 2006.